International Journal of Innovative Engineering Applications

Journal homepage: https://dergipark.org.tr/ijiea

A COMPARATIVE INVESTIGATION ON THE WEAR PERFORMANCE OF COMPACTED GRAPHITE IRON (CGI) TREATED WITH SINGLE AND DOUBLE TEMPERING

Engin Tan*[*1]*

[1]*Pamukkale University, Faculty of Technology, Department of Metallurgical and Materials Engineering, 20160, Kınıklı, Denizli, Türkiye*

Abstract

Original scientific paper

Compacted graphite iron (CGI) is a critical material in today's automotive and manufacturing industries. Heat treatment processes can improve CGI wear properties, related primarily to microstructural changes. In this study, single and double tempering heat treatments were carried out to improve the wear properties of CGI. Oil quenching was performed after 90 minutes of austenitization at 900°C, followed by 60 minutes of single and double tempering at three different temperatures (315, 350, and 375°C). The wear performance of the samples was compared using a pin-on disc test and hardness measurements. The volume loss and friction coefficient were evaluated, and wear maps were constructed to determine the samples' wear behavior. SEM and EDS analyses were carried out to worn surfaces to interpret the wear mechanisms. According to the study's findings, double tempering heat treatment may optimize wear performance better than traditional single tempering, and structures with high toughness-wear resistance combinations can be obtained.

Keywords: *Compacted graphite iron, double tempering, wear, hardness, scanning electron microscope.*

TEK VE ÇİFT TEMPERLEME İŞLEMİ YAPILMIŞ VERMİKÜLER DÖKME DEMİRİN (VDD) AŞINMA PERFORMANSI ÜZERİNE KARŞILAŞTIRMALI BİR ARAŞTIRMA

Özet

Orijinal bilimsel makale

Vermiküler dökme demir (VDD), günümüzün otomotiv ve imalat endüstrilerinde kritik bir malzemedir. Isıl işlem süreçleri, büyük ölçüde mikroyapısal değişikliklerle ilgili olan VDD aşınma özelliklerini iyileştirebilmektedir. Bu çalışmada, VDD'nin aşınma özelliklerini iyileştirmek için tek ve çift temperleme ısıl işlemleri gerçekleştirilmiştir. 900°C'de 90 dakikalık östenitleme ve yağda su vermeden sonra üç farklı sıcaklıkta (315, 350 ve 375°C) 60 dakika süreyle tek ve çift temperleme uygulanmıştır. Numunelerin aşınma performansı, pin-on disk testi ve sertlik ölçümleri kullanılarak karşılaştırılmıştır. Numunelerin aşınma davranışını belirlemek için hacim kaybı ve sürtünme katsayısı incelenmiş, ayrıca aşınma haritaları oluşturulmuştur. Aşınma mekanizmalarını yorumlamak için aşınma yüzeylerine SEM ve EDS analizleri uygulanmıştır. Çalışmanın bulgularına göre, çift temperleme ısıl işlemiyle aşınma performansının geleneksel tek tavlamaya göre daha iyi optimize edilebileceği ve yüksek tokluk-aşınma direnci kombinasyonuna sahip yapılar elde edilebileceği belirlenmiştir.

Anahtar Kelimeler: *Vermiküler dökme demir, çift temperleme, aşınma, sertlik, taramalı elektron mikroskobu.*

1 Introduction

Cast irons, which are widely used in industry, are essential alloys whose properties can be improved by heat treatment. Flake Graphite Iron (FGI), Nodular Graphite Iron (NGI), and Compacted Graphite Iron (CGI) are the most commonly used cast irons [1-4]. CGI has higher hardness and strength than FGI and better castability, machinability, and thermal conductivity than NGI. Therefore, CGI is used in components exposed to simultaneous mechanical, friction, and thermal loading, such as exhaust manifolds, cylinder heads and engine blocks in the automotive industry, and hydraulic bearings in the manufacturing industry [5-9].

The demand for high specific strength (strength/density) is growing as lightweight becomes more significant in the automotive industry. Despite having a higher density than aluminium alloys, CGI is lighter than FGI and NGI in components such as internal combustion engines, cylinder heads, and clutch pressure plates, where wear is a factor. It is therefore appealing in terms of utilization [10-13].

Heat treatment techniques improve the wear resistance of CGI components significantly. While the quenching process hardens CGI following austenitization, tempering is used to relieve the internal tensions at the operation's end. The tempering conditions can be optimized to achieve the best wear resistance [14-16].

* Corresponding author.

E-mail address: etan@pau.edu.tr (E. Tan)

Received 01 March 2022; Received in revised form 29 March 2022; Accepted 09 May 2022

Doi: https://doi.org/10.46460/ijiea.1081220

Many researchers investigate the wear behavior of different heat-treated parts in terms of various parameters to meet the industry's wear performance requirements [17-20]. According to the studies reviewed, heat treatment and manufacturing processes, in general, aim to optimize the surface hardness and wear characteristics of the components. Within this scope, in this study, single and double tempering methods were used to enhance the toughness-wear resistance combination of CGI. Double tempering has been demonstrated to be preferable in the industry for applications requiring both wear resistance and toughness. The effects of these techniques on the tribological properties of CGI were investigated in detail with microhardness measurements, wear tests and SEM-EDS analyses.

2 Experimental Procedure

CGI materials used in the study were commercially supplied by Döktaş Dökümcülük San. Tic. A.Ş., (Bursa, Türkiye). The chemical composition of CGI is given in Table 1, and the As-Cast hardness of 21.4 HRC. Cylindrical wear samples of 10x20 mm (Figure 1) were prepared from these As-Cast materials according to the ASTM G99 standard [21]. These samples were then subjected to a series of hardening and tempering heat treatment processes.

Table 1. Chemical composition of CGI (wt. %).

C	Si	Mn	P	S	Cr	Ni	Fe
3.73	2.47	0.35	0.011	0.013	0.035	0.019	Bal.

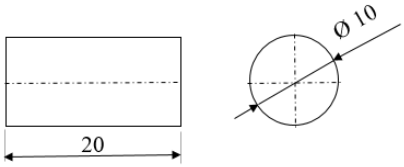

Figure 1. The dimensions of wear test sample.

The samples were first austenitized at 900°C for 90 minutes and then quenched in oil. After quenching in oil, single and double tempering processes were applied for 60 minutes at 315, 350, and 375°C temperatures. Finally, the samples were cooled in the air. The applied heat treatment program is given in Figure 2.

After heat treatments, surface oxide residues were removed by sanding and polishing. The samples' hardness was measured on the Rockwell C scale (HRC) according to the ASTM E18 standard before the wear tests [22]. Hardness measurement was performed on a Matsuzawa DXT-3 Rockwell hardness tester given in Figure 3 a.

Abrasive wear tests were carried out on a pin-on-disc wear device following ASTM G99 under 5, 10, and 15 N loads at 3 m/s sliding speed. Sliding distances are determined as 100, 200, and 300 m. Three samples were used for each parameter in the tests. Wear tests were performed on a Turkyus PODWT pin-on-disc test device given in Figure 3 b.

Figure 3. a) Hardness, b) Wear test devices used in the study.

Worn surfaces were analysed using the scanning electron microscope (Zeiss SUPRA 40VP) in the Advanced Technology Application and Research Center at Pamukkale University (Türkiye).

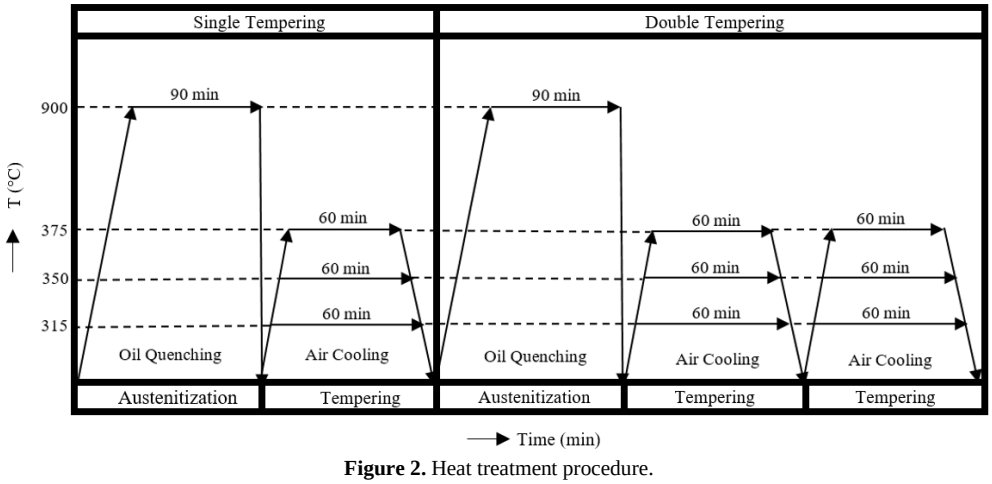

Figure 2. Heat treatment procedure.

3 Results and Discussion

The average hardness values of as-cast, quenched, and single/double tempered samples are given in Table 2 with standard deviations and hardness profiles in Figure 4. As the results show, the quenched sample had the maximum hardness value. The sample that was double tempered at 375°C had the lowest hardness. Single tempering has higher hardness values than double tempering at the same tempering temperatures. With higher tempering temperatures, the hardness of the samples gradually decreased. The images of the test samples before and after the wear tests in maximum load (15 N) were given in Figure 5.

Table 2. The average hardness values of the samples.

Sample	Hardness (HRC)	Standard Deviation
As-Cast	21.4	1.0
900-Quench	53.1	1.4
315-Single	48.7	0.2
315-Double	46.8	0.5
350-Single	43.9	0.6
350-Double	39.4	0.8
375-Single	35.3	0.9
375-Double	33.5	1.3

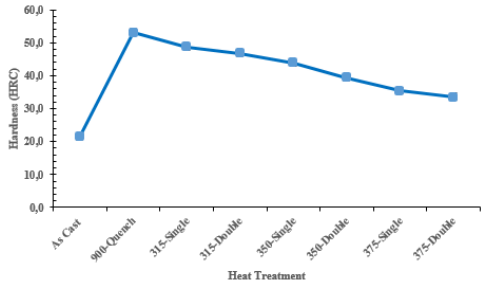

Figure 4. Hardness profile of As-Cast and heat-treated CGI.

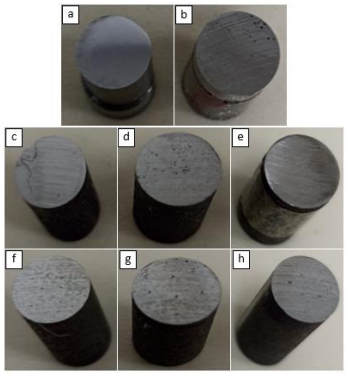

Figure 5. The images of the worn samples; a) As-Cast (before wear test), b) As-Cast, c) 315-Single, d) 350-Single, e) 375-Single, f) 315-Double, g) 350-Double, h) 375-Double.

Volume loss is one of the most critical factors in determining wear behavior. Figure 6 shows the effect of tempering heat treatment conditions on the wear behavior of CGI using volume loss graphs produced under various wear situations and heat treatment settings. Figure 6 clearly shows that the tempering heat treatment parameters and wear conditions directly affect the wear behavior. The highest volume loss was obtained in the As-Cast sample (Figure 6 a). Low hardness values can explain this high volume loss [23]. When the tempered samples are compared within themselves, it is seen that the highest wear resistance is obtained in the 315-Single sample (Figure 6 c). The decrease in wear resistance in other tempered specimens is due to the increased tempering temperature [24].

On the other hand, it was determined that the abrasion resistance of all tempered samples was higher than that of the As-Cast sample. The presence of carbide structures formed in the structure due to tempering causes an increase in hardness, which causes a significant increase in wear resistance [25-26]. The high wear resistance was determined when comparing the double tempered and single tempered samples. On the other hand, it was determined that there was not a very high decrease in wear resistance despite the decrease in hardness. This result shows that double tempering heat treatment can obtain structures with a high toughness-wear resistance combination.

Wear conditions, such as tempering parameters, also directly affect the volume loss. It is observed that the volume loss increases significantly with increasing sliding distance and load. This result agrees with the results of the studies in the literature [27].

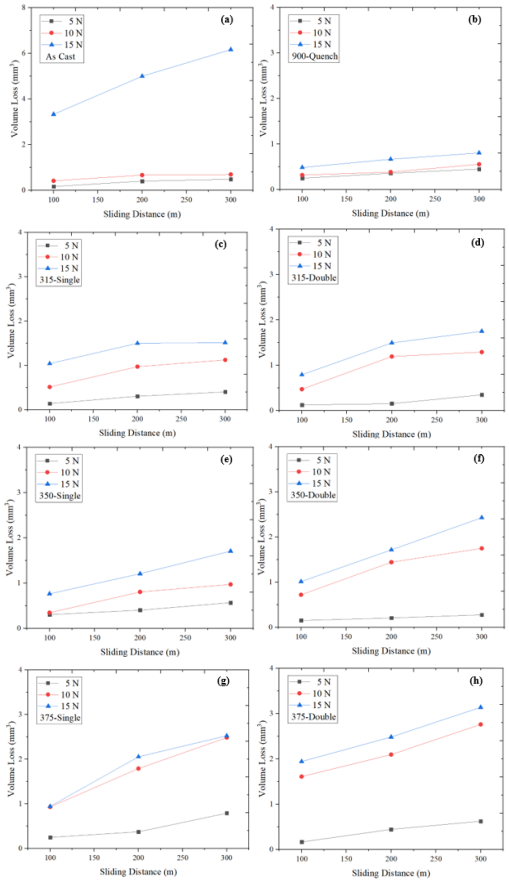

Figure 6. Effect of tempering conditions and wear parameters on the volume loss of CGI: a) As-Cast, b) 900-Quench, c) 315-Single, d) 315-Double, e) 350-Single, f) 350-Double, g) 375-Single, d) 375-Double.

Another parameter studied to determine the effect of tempering heat treatment parameters on the wear resistance of CGI is the coefficient of friction (Figure 7).

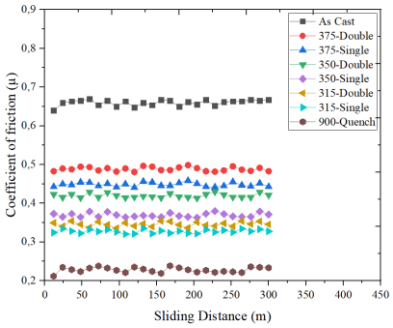

Figure 7. Effect of tempering conditions and wear parameters on the coefficient of friction of CGI.

Figure 7 clearly shows that the tempering parameter has a significant effect on the coefficient of friction of CGI. Among the tempered samples, the 315-Single sample (0.32) has the lowest coefficient of friction. The low coefficient of friction of the 315-Single samples

compared to the cast samples (0.65) can be explained by the significant increase in the hardness of the samples as a result of quenching and tempering heat treatment [28]. For comparison, the friction coefficients of the plain quenched samples (900-Quench) were investigated. 900-Quench specimens have the lowest coefficient of friction among all the specimens due to their high hardness. On the other hand, the As-Cast samples showed the highest friction coefficient values due to low hardness and the absence of carbides in the structure. This result shows conformity with previous studies [29-32].

In order to determine the effect of tempering heat treatment conditions on the wear mechanisms of CGI, wear maps of 315-Single and 315-Double samples were created (Figure 8). When Figure 8 is examined, the micro-cutting wear mechanism is dominant at low load and sliding distances, while micro-fracture and fatigue mechanisms are seen as more effective with increasing sliding distance and load. Fatigue mechanisms are affected by the interface temperature formed at the sample and abrasive interface [33]. It has been determined that double and single tempering directly affects the wear mechanisms. While less fatigue mechanism is observed in the 315-Double sample than in the 315-Single sample, a higher rate of micro-cutting wear mechanism is encountered at low forces.

Wear mechanisms directly affect wear resistance. In order to determine the effects of tempering and wear conditions on the wear behavior and removal mechanisms of CGI, SEM characterization of the worn surfaces was carried out. It is observed that the depth and width of the wear lines increase with increasing tempering temperature. The decrease explains this result in hardness with the increase of tempering temperature [34]. The highest wear marks were observed in the As-Cast sample, while the shallowest lines were obtained in the 900-Quench sample.

Similarly, the shallowest lines among the tempered samples were obtained in the 315-Single samples. It was observed that cracks especially started from areas close to graphite. This result agrees with the literature [35-36]. The wear mechanisms determined that the wear was realized with micro-cutting, micro-fracture, and fatigue mechanisms [Figure 9 to 13].

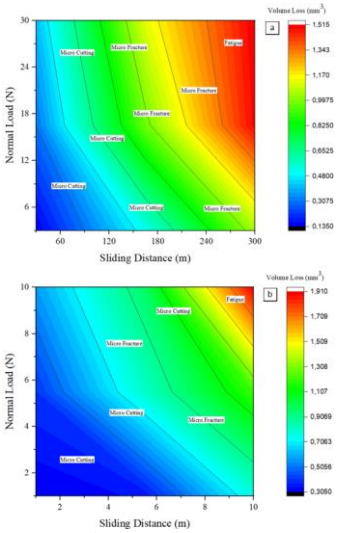

Figure 8. Wear map of; a) 315-Single, b) 315-Double samples.

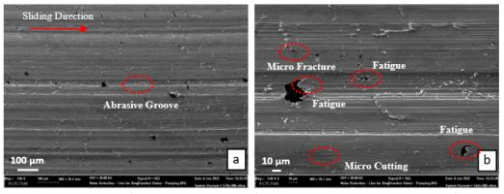

Figure 9. Worn surface analysis of As-Cast samples as a function of wear condition; a) X250, b) X1000.

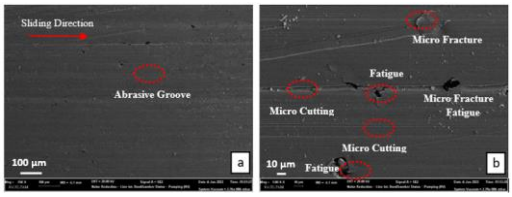

Figure 10. Worn surface analysis of quenched samples as a function of wear and tempering condition; a) X250, b) X1000.

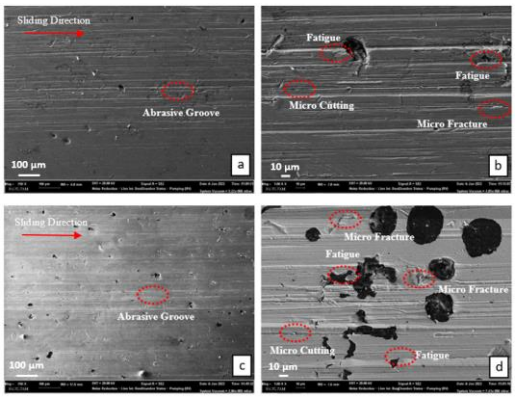

Figure 11. Worn surface analysis of tempered samples as a function of wear and tempering condition; a)375-Single X250, b) 375-Single X1000, c)375-Double X250, d) 375-Double X1000.

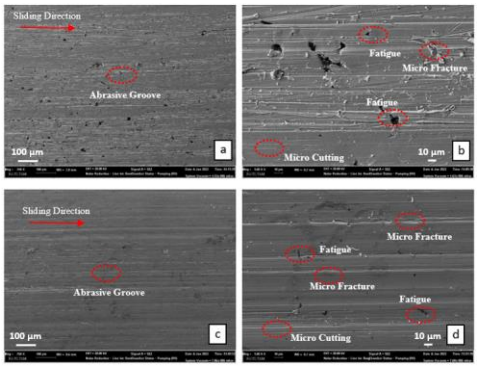

Figure 12. Worn surface analysis of tempered samples as a function of wear and tempering condition; a)350-Single X250, b) 350-Single X1000, c)350-Double X250, d) 350-Double X1000.

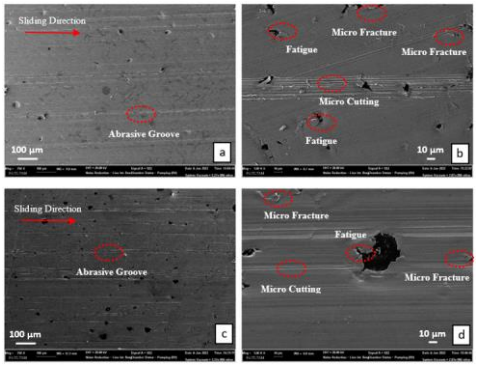

Figure 13. Worn surface analysis of tempered amples as a function of wear and tempering condition; a)315-Single X250, b) 315-Single X1000, c)315-Double X250, d) 315-Double X1000.

EDS analysis was used to determine the elemental distribution on the surface of the 315-Single sample with the best wear resistance (Figure 14). It was found that the distributions of Fe, Si, and C were homogeneous by the chemical composition of CGI. The elemental distribution is seen to be consistent with the literature [12, 14, 24].

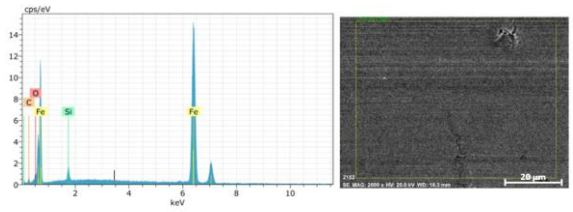

El	AN	Series	unn. C [wt.%]	norm. C [wt.%]	Atom. C [at.%]	Error (1 Sigma) [wt.%]
Fe	26	K-series	87.01	90.99	72.59	2.36
C	6	K-series	4.47	4.67	17.33	1.12
O	8	K-series	2.56	2.67	7.44	0.55
Si	14	K-series	1.59	1.66	2.64	0.10
		Total:	95.62	100.00	100.00	

Figure 14. EDS analysis worn surface of 315-Single sample.

4 Conclusion

Double tempering heat treatment will optimize toughness and wear and provide higher wear performance at a more affordable cost in the industry for CGI materials. The results of the study carried out in this context are presented below:

- As a result of tempering processes, the highest hardness was obtained in the 315-Single sample with 53.1 HRC, while the lowest hardness was observed in 33.5 HRC and 375-Double samples. While the hardness decreased as the tempering temperature increased, higher hardness was obtained in single tempering compared to double tempering for equivalent temperatures.
- The highest volume loss was obtained in the As-Cast sample in the wear tests. It was observed that the highest wear resistance among the tempered samples was obtained in the 315-Single sample. When the double tempered samples were compared with the single tempered samples, it was determined that they had higher wear resistance. On the other hand, despite the decrease in hardness, it was observed that there was not a very high decrease in wear resistance. This result showed that double annealing heat treatment could obtain structures with a high toughness-wear resistance combination.
- Among the tempered samples, the 315-Single sample has the lowest coefficient of friction with 0.32. 900-Quench samples have the lowest coefficient of friction among all specimens due to their high hardness. As-Cast samples showed the highest coefficient of friction with 0.65.
- The highest wear marks were observed in the As-Cast sample, while the shallowest lines were obtained in the 900-Quench sample. The shallowest lines among the tempered samples were obtained in the 315-Single samples.
- It has been determined that wear is realized by micro-cutting, micro-fracture, and fatigue mechanisms as wear mechanisms.

Acknowledgments

The author is thankful to Dr. İsmail Ovalı for his contributions to the study.

Declaration

Ethics committee approval is not required.

References

[1] Ovalı, İ. (2012). *Chill formation on the surface of ductile iron and the effects of austempering heat treatments on microstructures and mechanical properties.* (Doctoral dissertation, Gazi University).

[2] Tooptong, S., Park, K. H., & Kwon, P. (2018). A comparative investigation on flank wear when turning three cast irons. *Tribology International*, 120, 127-139.

[3] Kayalı, Y. (2016). Effect of different heat treatments on mechanical properties of ductile iron. *Afyon Kocatepe University Journal of Science and Engineering*, 16(1), 192-197.

[4] Toktaş, G., Toktaş, A. (2018). Carbidic austempered ductile irons. *Journal of Balikesir University Institute of Science and Technology*, 20(1), 13-21.

[5] Pina, J. C., Shafqat, S., Kouznetsova, V. G., Hoefnagels, J. P. M., & Geers, M. G. D. (2016). Microstructural study of the mechanical response of compacted graphite iron: An experimental and numerical approach. *Materials Science & Engineering A*, 658, 439-449.

[6] Sjogren, T., Vomacka, P., & Svensson, I. L. (2004). Comparison of mechanical properties in flake graphite and compacted graphite cast irons for piston rings. *International Journal of Cast Metals Research*, 17(2), 65-71.

[7] Dawson, S. (2009). Compacted graphite iron-A material solution for modern diesel engine cylinder blocks and heads. *China Foundry*, 6, 241-246.

[8] Yang, W. J., Pang, J. C., Wang, L., Wang, S. G., Liu, Y. Z., Hui, L., Li, S. X. & Zhang, Z. F. (2021). Tensile properties and damage mechanisms of compacted graphite iron based on microstructural simulation. *Materials Science & Engineering A*, 814, 141244.

[9] Nayyar, V., Kaminski, J., Kinnander, A., & Nyborg, L. (2012). An experimental investigation of machinability of graphitic cast iron grades; flake, compacted, and spheroidal graphite iron in continuous machining operations. *Procedia CIRP*, 1, 488-493.

[10] Slatter, T., Lewis, R., & Jones, A. H. (2011). The influence of induction hardening on the impact wear resistance of compacted graphite iron (CGI). *Wear*, 3-4, 302-311.

[11] Dawson, S., & Indra, F. (2014). Compacted graphite iron-a new material for highly stressed cylinder blocks and cylinder heads. *Sintercast*, 1-14.

[12] Ki, S., Cockcroft, S. L., Omran, A. M., & Hwang, H. (2009). Mechanical, wear and heat exposure properties of compacted graphite iron at elevated temperatures. *Journal of Alloys and Compounds*, 487, 253-257.

[13] Lewis, R., & Dwyer-Joyce R. S. (2002). Wear diesel engine inlet valves and seat inserts. *Journal of Automobile Engineering Proceedings of the IMechE Part D*, 216, 205-216.

[14] Venugopal Rao, S., Venkata Ramana, M., & Kumar, A. C. S. (2019). An experimental investigation on compact graphite iron wear behavior at 32 °C and 200°C. *Materials Today: Proceedings*, 19, 778-780.

[15] Ovalı, İ., & Mavi, A. (2011, May) The effect of ausferrite volume fraction on the surface roughness of dual-phase matrix structure ductile iron. *Proceedings of the 6th International Advanced Technologies Symposium/Elazig.* (pp. 156-160).

[16] Venugopal Rao, S., Venkata Ramana, M., & Kumar, A. C. S. (2021). Friction and dry sliding wear properties of compact graphite iron at room temperature and 100 °C. *Materials Today: Proceedings*, 45, 3250-3254.

[17] Kaplan, Y., Yıldırım, A., & Aksöz, S. (2020). The effect of oxidation process after nitrocarburization on tribological properties of AISI 4140 steel. *Journal of Polytechnic*, 23(4), 1357-1362.

[18] Pamuk, Ö., Kaplan, Y., & Aksöz, S. (2022). The effects of different heat treatment regimes on the wear properties of Fe-based composite materials. *Powder Metallurgy and Metal Ceramics, 60(7-8)*, 439-450.

[19] Federici, M., Cinzia, M., Moscatelli A., & Gialanella, S. (2017). Pin-on disc study of a friction material dry sliding against HVOF coated discs at room temperature and 300 °C. *Tribology International*, 115, 89-99.

[20] Filho, D. D. S., Tschiptschin, A. P., & Goldenstein, H. (2018). Effects of ethanol content on cast iron cylinder wear in a flex-fuel internal combustion engine–A case study. *Wear*, 406-407, 105-117.

[21] Annual book of ASTM standards. (2017). *Standard test method for wear testing with a pin-on-disk apparatus* (ASTM G99-17).

[22] Annual book of ASTM standards. (2005). *Standard test method for Rockwell Hardness and Rockwell Superficial Hardness of metallic materials* (ASTM E18).

[23] Woodward, R. G., Toumpis, A., & Galloway, A. (2022). The influence of tempering and annealing on the microstructure and sliding wear response of G350 grey cast iron. *Wear*, 496-497, 204283.

[24] Wang, B., Qiu, F., Zhang, Y., Yang, J., Cui, W., Jin, Y., Cai, G., Yuan, Y., Guo, S., Li, H., & Barber, G. C. (2022). Influences of dual-phased nanoparticles on microstructure, mechanical properties and wear resistance of vermicular graphite cast iron. *Materials Letters*, 308-b, 131296.

[25] Masuda, K., Oguma, N., Ishiguro, M., Sakamoto, Y., & Ishihara, S. (2021). Sliding wear life and sliding wear mechanism of gray cast iron AISI NO.35B. *Wear*, 474-475, 203870.

[26] Öztürk, E., & Yıldırım, M. (2019). Effect of austempering temperature and time on microstructure and hardness of austempered ductile cast irons (ADI). *Konya Journal of Engineering Sciences*, 7(3), 604-611.

[27] Akinribide, O. J., Akinwamide, S. O., Obadele, B. A., Ogundare, O. D., Ayeleru, O. O., & Olubambi, P. A. (2021). Tribological behaviour of ductile and austempered grey cast iron under dry environment. *Materials Today: Proceedings*, 38, 1174-1182.

[28] Wang, B., Pan, Y., Liu, Y., Lyu, N., Barber, G. C., Wang, R., Cui, w., Qiu, F., & Hu, M. (2020). Effects of quench-tempering and laser hardening treatment on wear resistance of gray cast iron. *Journal of Materials Research and Technology*, 9(4), 8163-8171.

[29] Torre, U. D. L., Gonzalez-Martinez, R., & Mendez, S. (2020). Effect of the section size, holding temperature, and time on the kinetics of the ausferritic transformation and mechanical properties of as-cast ausferritic ductile iron. *Materials Science and Engineering: A*, 788, 139536.

[30] Li, Y., Song, R., Chen, C., Zhao, Z., & Pei, Y. (2019). Enhancing mechanism of interaction of individual phases of 3.45 wt%Cr–Mn–Cu–Ni–B iron after quenching and tempering. *Materials Science and Engineering: A*, 760, 165-173.

[31] Cui, J., & Chen, L. (2017). Microstructure and abrasive wear resistance of an alloyed ductile iron subjected to deep cryogenic and austempering treatments. *Journal of Materials Science & Technology*, 33(12), 1549-1554.

[32] Çetin, M., & Gül, F. (2007). Effect of the matrix structure on the friction coefficient and pin temperature of ductile iron under dry sliding conditions. *Journal of Gazi University Faculty of Engineering and Architecture*, 22(3), 273-280.

[33] Wang, B., Pan, Y., Barber, G. C., Qiu, F., & Hu, M. (2020). Wear behavior of composite strengthened gray cast iron by austempering and laser hardening treatment. *Journal of Materials Research and Technology*, 9(2), 2037-2043.

[34] Vadiraj, A., Balachandran, G., Kamaraj, M., & Kazuya, E. (2011). Mechanical and wear behavior of quenched and tempered alloyed hypereutectic gray cast iron. *Materials & Design*, 32(4), 2438-2443.

[35] Coronado, J. J., Gomez, A., & Sinatora, A. (2009). Tempering temperature effects on abrasive wear of mottled cast iron. *Wear*, 267(11), 2070-2076.

[36] Gecü, R. (2022). Investigation of the effects of aluminum addition and austempering heat treatment on wear behavior of ductile cast irons. *Niğde Ömer Halisdemir University Journal of Engineering Sciences*, 11(2), 1-1.